Influence of chemical environment on resonant core excitation of C(1*s*) in CO_2, OCS, and CS_2 by electron impact

T. Kroin, S. E. Michelin, A. S. Falck, and F. Arretche
Departamento de Física, UFSC, 88040-900 Florianópolis, Santa Catarina, Brazil

M.-T. Lee and Ione Iga
Departamento de Química, UFSCar, 13565-905 São Carlos, São Paulo, Brazil
(Received 16 December 2002; published 2 July 2003)

In this work, we report a theoretical study of the role played by chemical environment on the electron-impact resonant core excitations in OCS, CO_2, and CS_2 molecules. Calculated differential and integral cross sections for the promotion of a carbon 1*s* electron to the lowest unfilled $p\pi$ orbital of these molecules, or more specifically, the ratios of these cross sections for the corresponding transitions leading to the singlet and the triplet core-excited states in the 300–800 eV incident energy range, are reported. The distorted-wave approximation was applied to these calculations. Our study revealed resonance structures in the calculated ratios for CO_2, in good agreement with the available experimental observation, which is very encouraging. On the other hand, no resonance structure is clearly seen in the calculated ratios for OCS and CS_2 molecules. The possible reason for the nonappearance of resonance for these two targets is discussed.

DOI: 10.1103/PhysRevA.68.012701 PACS number(s): 34.80.Gs

I. INTRODUCTION

The occurrence of shape resonance is commonly observed in low-energy electron collisions, photoabsorption, and photoionization processes involving molecules both isolated and/or adsorbed on surfaces. Typically, this phenomenon can be characterized by an enhancement of the cross sections about the energy region where the resonance happens. In the past 20 years, almost miraculous capacities were attributed to shape resonances [1], in particular the application on the determination of bond lengths of molecules adsorbed on surfaces by extended x-ray-absorption fine-structure (EXAFS) like techniques [2,3]. Physically speaking, this enhancement of the cross sections can be well described by the trapping of an outgoing electron by a potential barrier through which the electron eventually tunnels and emerges in the continuum [4–6]. In this qualitative picture, the details of the molecular potential, formed by interplay of attractive and repulsive forces, are shaped in such a way as to support a temporary bound electronic state. Therefore, it is typically a one-electron phenomenon. If the model based on a potential barrier is used to explain the occurrence of shape resonances, it would be very difficult to correlate directly the complicated details of the molecular potential and bond lengths. Nevertheless, such a correlation does exist and can be clearly seen when one plots the energy dependence of electron-molecule-scattering eigenphase sums as a function of internuclear distances [7].

An alternative model treats shape resonance as arising from scattering process by neighboring atoms. Indeed, the latter model is supported by an empirical linear relationship which correlates the energy position of the resonance and the molecular bond lengths between a determined atom and its neighbors [8,9]. The existence of such a one-to-one relationship would allow, in fact, the determination of bond lengths of adsorbed molecules via the so-called bond-length-with-a-ruler method. However, for molecules such as CO, CO_2, and H_2CO, etc., more than one *K* edge is observed. The shape resonance distance from the threshold is not necessarily the same at both edges, thus it is not clear which value to choose in the correlation with bond lengths. Usually, an average position has been chosen in the NEXAFS literature with questionable physical meaning [1].

Moreover, the structure determination of molecules adsorbed on surface requires a correct assignment of the resonance positions. Nevertheless, such assignment remains a difficult task, not only because of the broadness of the resonance but also due to the fact that the shape resonance is not the only physical phenomenon leading to a visible enhancement in the cross sections. In fact, the enhancements of cross sections can also originate from multielectron processes such as double-excited states and satellite thresholds, which are actually nonresonant phenomena.

An interesting aspect is that the shape resonance can also occur in electron-impact core-excitation processes of molecules. In this case, the low-energy outgoing electron can be trapped by the potential barrier of the excited target, which leads to the formation of temporary negative ions associated with inner-shell-excited molecules. Such resonances were observed for several molecules as structures in the positive ion yields, resulting from electron impact on molecules. They were also observed by Zeisel *et al.* [10] and Teillet-Billy and Zeisel [11] in investigations on individual positive-ion decay channels by mass-spectroscopic analysis of the reaction products. More recently, the formation of an inner-shell-excited negative temporary ion was also attributed by Harrison and King [12] to explain the observed resonance-like structure in the measured ratios of the total excitation intensities for singlet and triplet ($C_{1s}\sigma \rightarrow 2p\pi$) transitions in CO. A similar structure was also observed by Blount and Dickinson [13] in the ratio of differential excitation intensities of the $(C_{1s})^{-1}(2p\pi_u)$, $^{1,3}\Pi_u$ states of CO_2 by electron

impact at incident energies near 313 eV. The existence of such structures in electron-impact core excitation of molecules would be interesting, in particular, if an empirical one-to-one (resonance position)/(bond length) relationship could also be verified. Although a direct application such as for adsorbed molecule structure determination using inner-shell electron energy-loss spectroscopy (EELS) is unlikely due to the weakness of the core loss inelastic scattering signals, it may have some practical application in the gas-phase inner-shell EELS studies.

From a chemical point of view, the highly localized carbon *K*-shell electrons in all small molecules are essentially atomic, and therefore their wave functions are expected to be very similar to each other. On the other hand, the formation of the *K* shell excited temporary negative ions would depend on the outer valence electronic structure, in particular the height and shape of the potential barrier of each molecule. Indeed, the bond-length correlation has shown that C-S and C-O bonds give rise to different resonance behavior: while the former is in the discrete, the latter is situated in the continuum [14]. Therefore, investigations on the influences of chemical environment on resonant electron-impact core-excitation processes of molecules are certainly very interesting.

Despite the increasing experimental interest in electron-impact core excitation of molecules, very few theoretical studies on this field were reported in the literature. Although a solid-based *ab initio* multichannel study on this matter is desirable, computationally, the coupling between the high-energy incident electron and the low-energy exit electron is very difficult to deal with. For this reason, the distorted-wave approximation (DWA) is presently the most reliable theoretical method for such studies. Although the interchannel coupling effects are not taken into account by this theoretical formulation, the shape resonance phenomenon, i.e., the temporary trapping of the low-energy scattering electron by the potential barrier of the excited target, is represented in the collisional dynamics. Therefore, a comparison between calculated and experimental resonance line shape may provide an indication of the importance of interchannel couplings. Recently, the DWA was applied in the studies of carbon *K*-shell core-excitation processes of CO_2 [15] and CO [16] by electron impact. The comparison between the calculated results and the available experimental data is encouraging. In the present work, we extend the application of the DWA to study the electron-impact excitation of carbon *K*-shell electrons in OCS, CO_2, and CS_2 molecules to the lowest unfilled $p\pi$ orbitals. A comparison of the calculated excitation cross sections for the singlet and triplet $(C_{1s}\sigma)^{-1}(p_\pi)$ transitions in these molecules, or more specifically, the ratios of the differential cross sections, RD(1:3), and the integral cross sections, RI(1:3), for these transitions as a function of incident energies would provide insight into the dynamics of core-excitation processes.

The organization of the present paper is as follows. In Sec. II, an outline of the theory used is presented in which we also give some details of the calculations. In Sec. III, we present our calculated data and summarize our conclusions.

II. THEORY AND CALCULATION

Since the detail of the basic theory used has already been presented elsewhere [17–20], it will only be briefly described here. The differential excitation cross sections (DCS's) for electron-molecule scattering averaged over molecular orientations are given by

$$\frac{d\sigma}{d\Omega}=\frac{1}{8\pi^2}\int d\alpha \sin\beta d\beta d\gamma |f(\hat{k}_f')|^2, \tag{1}$$

where $\hat{k}_f'$ is the direction of the scattered electron linear momentum in the laboratory frame (LF), whereas the direction of the incident electron linear momentum is taken as zero. The (α,β,γ) are the Euler angles, which define the direction of the molecular principal axis in the LF. The body-frame (BF) amplitude $f(\hat{k}_i,\hat{k}_f)$ is related to the *T*-matrix elements by the formula

$$f(\hat{k}_i,\hat{k}_f)=-2\pi^2 T_{if}. \tag{2}$$

Within the DWA framework, the transition *T* matrix is given by

$$T_{if}=\langle \varphi_1 \Psi_{k_f}^{(-)}|U_{se}|\varphi_0\Psi_{k_i}^{(+)}\rangle, \tag{3}$$

where φ_0 and φ_1 are the initial and final target wave functions, respectively. These wave functions are Slater determinants with appropriate symmetries. $\Psi_{k_i}^{(+)}$ and $\Psi_{k_f}^{(-)}$ are the initial and final distorted continuum wave functions with the outgoing- $(+)$ and incoming-wave (-) boundary conditions, respectively. U_{se} is the static-exchange potential operator. The distorted wave functions are solutions of the Lippmann-Schwinger equation,

$$\Psi_{i,f}^{(\pm)}=\Phi_{i,f}+G_0^{(\pm)}U_{i,f}\Psi_{i,f}^{(\pm)}, \tag{4}$$

where $G_0^{(\pm)}$ is the free-particle Green's operator with appropriate boundary condition, and $\Phi_{i,f}$ are the plane-wave functions associated with the initial *i* and the final *f* states, respectively. For the calculation of the initial and the final distorted-wave functions $\Psi_{i,f}$, the static-exchange fields generated from the ground-state and the excited-state target wave functions, respectively, were used. The Schwinger variational iterative method (SVIM) [21] was applied to solve the corresponding Lippmann-Schwinger scattering equation. Although the continuum orbitals of the incoming electron are known to be orthogonal to all orbitals of the ground-state target, it is not true for the wave functions of the scattered electron since they are calculated in the static-exchange field of an open-shell target. For simplicity of the calculation, these outgoing orbitals were constrained to be orthogonal to all occupied orbitals in the final-state target wave functions. The same procedure was also applied in our previous study for CO [16].

The ground-state configuration of the molecules is represented by a single-determinant near-Hartree-Fock wave function. This wave function is generated by a self-consistent-field (SCF) calculation using a standard $[11s6p]/[5s3p]$

TABLE I. Additional basis functions used in the SCF calculations.

Molecule	Center	Basis functions	Exponents
CO_2	C	s	0.0453, 0.0157, 0.005 37
		p	0.0323, 0.007 34
		d	1.373, 0.523
	O	*s*	0.0853, 0.0287, 0.004 73
		p	0.0551, 0.0183, 0.003 111
		d	1.471, 0.671
OCS	C	*s*	0.0453, 0.0157, 0.0051
		p	0.032 37, 0.009 31
		d	1.373, 0.433
	O	*s*	0.0433, 0.0151, 0.0073
		p	0.091 16, 0.032 32, 0.008 33
		d	1.433, 0.311
	S	*s*	0.0459, 0.0171, 0.0087
		p	0.0502, 0.0173
		d	1.539, 0.344
CS_2	C	*s*	0.0537, 0.0157, 0.004 53
		p	0.032 37, 0.009 34
		d	1.673
	S	*s*	0.0459, 0.0178
		p	0.0502, 0.0153
		d	1.533

[a]Cartesian Gaussian basis functions are used. They are defined as $\phi^{\alpha,\ell,m,n,\mathbf{A}}(\mathbf{r})=N(x-\mathbf{A}_x)^{\ell}(y-\mathbf{A}_y)^m(z-\mathbf{A}_z)^n\exp(-\alpha|\mathbf{r}-\mathbf{A}|^2)$, with N a normalization constant.

contracted Gaussian basis of Dunning [22] for carbon and oxygen atoms, and a standard $[11s7p]/[6s4p]$ contracted basis of Huzinaga [23] for sulfur atom. These basis sets were augmented by some uncontracted Cartesian Gaussian functions in the SCF calculations. The additional functions for each molecule are shown in Table I. At the experimental equilibrium geometries, these basis sets provide SCF energies of -187.707 a.u., -510.2988 a.u., and -832.85 a.u. for CO_2, OCS, and CS_2 molecules, respectively. These values are in good agreement with calculated SCF energies reported in the literature [24–26].

The same basis sets are also used to generate the wave functions of the excited states using the improved virtual orbital (IVO) approximation [27] by diagonalizing the V_{N-1} potential of the core in the SCF basis. A brief comparison of our calculated vertical excitation energies for the $C_{1s}\rightarrow{}^{1,3}\Pi$ transitions as well as the singlet-triplet energy splitting with the available calculated [28] and experimental data [12,29] are shown in Table II. It is seen that the calculated vertical excitation energies by the IVO approximation are in general 7–10 eV above the experimental values for these three molecules, which is quite reasonable. The agreement between the calculated and experimental singlet-triplet energy splitting is also fair. The experimental excitation thresholds were used in the calculation of the cross sections in the present study.

TABLE II. Vertical excitation energies (ΔE) and singlet/triplet energy shifts (δ).

Molecule	ΔE for $C_{1s}\rightarrow{}^1\Pi$ (eV)	ΔE for $C_{1s}\rightarrow{}^3\Pi$ (eV)	δ (eV)
CO_2	298.57	296.36	2.21
	290.75 [a]	289.33 [a]	1.47 [b]
	301.7 [c]		
OCS	296.86	294.86	2.00
	288.23 [a]	287.10 [a]	1.13 [a]
CS_2	295.52	293.65	1.87
	286.10 [a]	285.20 [a]	0.90 [a]

[a]Experimental results of Harrison and King [12].
[b]Experimental results of Almeida *et al.* [29].
[c]Calculated data of Roberty *et al.* [28].

III. RESULTS AND DISCUSSION

In Fig. 1, we compare our calculated RI(1:3) in the 300–800-eV energy range for the electron-impact $(2\sigma_g\rightarrow 2\pi_g)$ singlet and triplet transitions in CO_2 with the experimental ratios of Almeida *et al.* [29]. Instead of detecting scattered electrons as in conventional EELS, the new technique used in the studies of Almeida *et al.* detects electrons that originated from the decay of autoionizing excited states, which are formed by promotion of a core electron to an empty

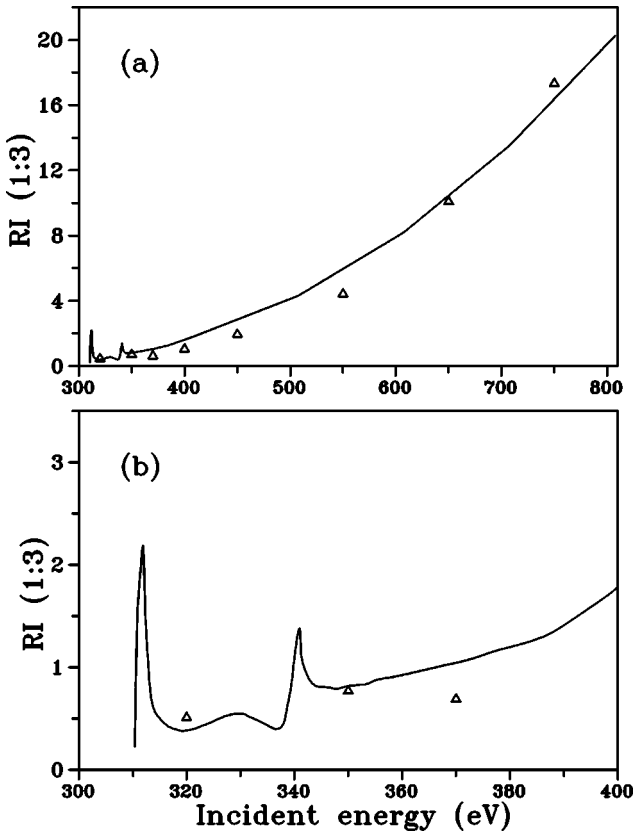

FIG. 1. RI(1:3) for electron-impact core excitations of CO_2 in the (a) 300–800-eV and (b) 300–400-eV energy ranges. Solid line, present calculated results; open triangles, measured relative results of Almeida *et al.* [29], normalized to our results at 350 eV.

valence orbital by electron impact. This technique brought some advantages, one of which was that high-resolution ejected electrons can be observed without an energy-selected electron gun, since their energies are well defined. Nevertheless, the intensity of ejected electrons that originated from autoionizing processes depends on two transition probabilities, namely that from the formation of excited states by electron impact and that from their subsequent decay. Although it is expected that the contribution arising from the decay is independent of impact energies, the efficiency of this process may depend on the spin nature (multiplicity) of the excited state. Therefore, their measured RI(1:3) are, in fact, not absolute and are proportional to the ratios between the electron-impact excitation cross sections leading to the $^3\Pi$ and $^1\Pi$ states. For this reason, their RI(1:3) are normalized to our calculated data at 350 eV. It is seen in Fig. 1(a) that there is a generally good agreement between the calculated and measured results. At energies below 350 eV, some resonancelike structures are seen in the theoretical results. These structures can be better visualized in Fig. 1(b), where we have limited the impact energy up to 400 eV. Two sharp resonance peaks, located at incident energies around 312 eV and 340 eV, respectively, are clearly seen. Nevertheless, no structures show up in the experimental data due to the fact that the energy mesh of their experiment is too sparse in this region. Indeed, only two experimental values of RI(1:3) are presented in the 300–350-eV energy range. This sparse energy spacing in the experimental data precludes the possibility of verifying the calculation.

In Fig. 2(a), we present our RD(1:3) in the 300–400-eV energy range, calculated at a scattering angle of 6° for the electron-impact $(2\sigma_g \rightarrow 2\pi_g)$ singlet and triplet transitions in CO_2. The corresponding experimental ratios of Blount and Dickinson [13] are shown as well for comparison. These results were taken at a determined small scattering angle using EELS. The RD(1:3) ratios were obtained directly by dividing intensities of the inelastically scattered electrons arising from the excitation to the singlet state by those corresponding quantities to the triplet state. In this sense, their measured RD(1:3) values are absolute and can be directly compared with our calculated data. Unfortunately, these authors did not reveal the scattering angle at which the data were taken. Since our calculation has shown no sensitive variation of the calculated RD(1:3) for scattering angles below 30°, the ratios calculated at 6° are arbitrarily chosen for comparison. It is seen that there is a very good qualitative agreement between our calculated ratios and the experimental results of Blount and Dickinson [13]. In particular, the resonance in the experimental data, located at incident energy of about 312 eV, is well reproduced in our calculations. The quantitative agreement between the calculated and experimental ratios is also fair, which is encouraging. In Fig. 2(b), a comparison between the calculated and experimental line shape of this resonance is shown. Although our resonance is slightly shifted toward lower incident energies, the two line shapes are quite similar, which may indicate that the singlet-triplet interchannel coupling is not very important. Also, it is interesting to note that the resonance appearing in our calculated RI(1:3) [Fig. 1(b)] at around 340 eV cannot be

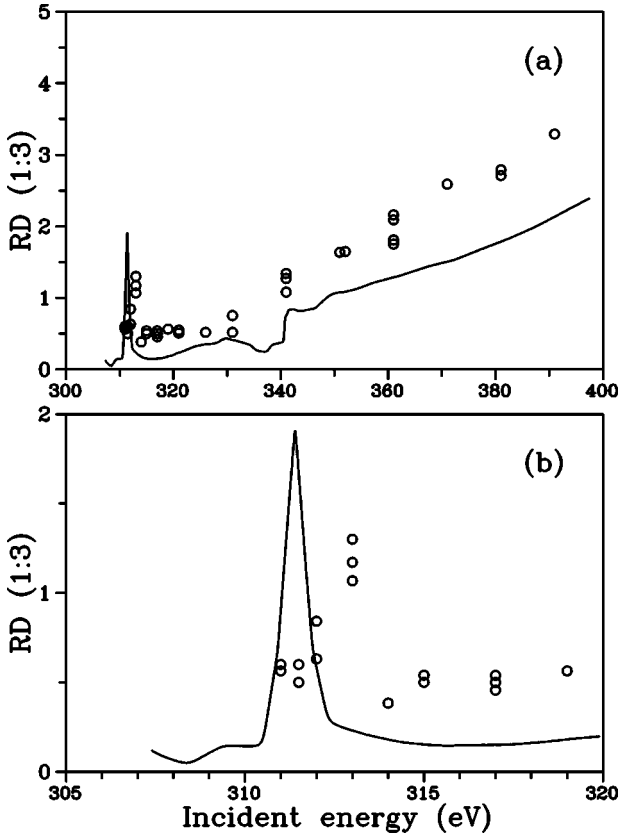

FIG. 2. RD(1:3) for electron-impact core excitations of CO_2 in the (a) 300–400 and (b) 305–320-eV energy range. Solid line, present results calculated at a scattering angle of 6°; open circles, measured ratios of Blount and Dickinson [13].

clearly identified in both theoretical and experimental RD(1:3). In order to understand this discrepancy, in Fig. 3 we present RD(1:3) in the 300–400 eV range, calculated for several scattering angles. In this figure, one observes that although the resonance feature at around 312 eV is very clear for all scattering angles, the one around 340 eV only becomes evident with increasing scattering angles. In order to understand the physical origin of these resonances, in Fig. 4 we present the partial integral cross sections (ICS's) for the four lowest, namely $^2\Sigma_g$, $^2\Sigma_u$, $^2\Pi_g$, and $^2\Pi_u$ scattering channels, as a function of incident electron energy for transitions leading to the singlet and triplet excited states in CO_2. Resonance structures are present in the partial ICS's for both singlet and triplet excitations. The sharp resonances (located at about 309 eV for triplet excitation and 312 eV for singlet excitation) are due to the $^2\Pi_u$ scattering channel while those located at about 340 eV are of the $^2\Sigma_u$ nature. An eigenphase-sum analysis (not shown) of these channels has also confirmed the above assignment. Therefore, the observed structure in the experimental RD(1:3) located at an impact energy of 312 eV can probably be associated with the $^2\Pi_u$ resonance. On the other hand, it is expected that the resonance structure in RD(1:3) near 340 eV, associated with the $^2\Sigma_u$ resonance, would only be observed at larger scattering angles.

Figure 5 compares the calculated RI(1:3) for electron-

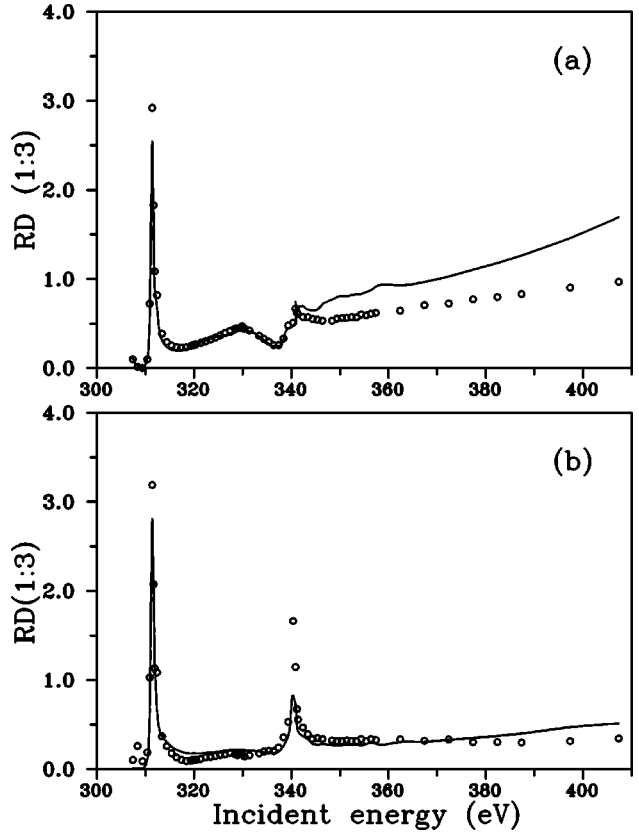

FIG. 3. Calculated RD(1:3) for electron-impact core excitations of CO_2 in the 300–400-eV energy range. In (a), solid line, present results at a scattering angle of 30°; open circles, at 60°. In (b), solid line, present results at a scattering angle of 120°; open circles, at 180°.

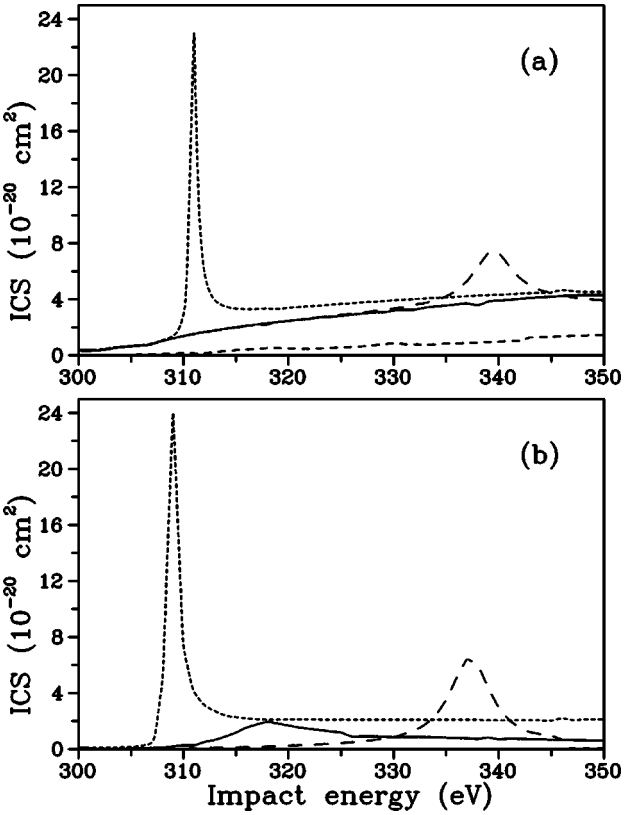

FIG. 4. Calculated partial ICS's for the four lowest e^--CO_2 scattering channels leading to (a) the singlet and (b) triplet excited states. Solid line, results for the $^2\Sigma_g$; dashed-line, for the $^2\Sigma_u$; short-dashed line, for the $^2\Pi_g$; and dotted line, for the $^2\Pi_u$ scattering channels.

impact excitation of a carbon *K*-shell electron to the lowest unoccupied π orbitals in CO_2, OCS, and CS_2 molecules in the 300–410-eV incident energy range. It is very interesting to note that, in the energy regions where no shape resonances are observed, the calculated ratios for these targets agree very well with each other, both qualitatively and quantitatively. This good agreement seems to indicate that the nonresonant electron-impact excitation of core $C(1s)$ electrons is practically independent of the valence-shell chemical environment of these molecules. On the other hand, the resonant core-excitation behavior of these molecules is very different. For CO_2, two sharp shape resonances at around 312 eV and 340 eV incident energies are clearly seen. For OCS, only a small bump near 342 eV incident energy is observed, which may indicate the existence of a shape resonance, while for CS_2 there is no evidence of resonance in the entire energy range. In order to understand the nonappearance of resonancelike structures in the calculated RI(1:3) for these two targets, in Figs. 6 and 7 we present the singlet and triplet partial excitation ICS's for some dominant scattering symmetries, as a function of impact energy, for e^--OCS and e^--CS_2 scatterings, respectively. These figures show in common a weak and very broad structure, located at about 317 eV, in the ICS's of $^2\Pi$ scattering channels in OCS and $^2\Pi_u$ channels in CS_2. Also, broad structures located at about 340 eV in the $^2\Sigma$ partial ICS's of OCS and located at about 337 eV in the $^2\Sigma_u$ partial ICS's of CS_2 can be easily identified. These structures are much weaker in magnitude than the corresponding ones in CO_2. Although the weakness of these structures can explain in part the different behavior of the RI(1:3) seen in CO_2 relative to the other two molecules, more importantly we have noticed that for e^--CO_2, the positions of the corresponding resonances for the singlet and triplet exci-

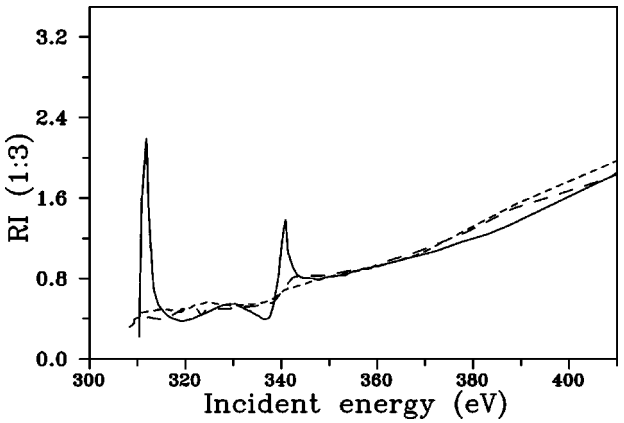

FIG. 5. Calculated RI(1:3) for electron-impact core excitations in the 300–410 eV energy range. Solid line, results for CO_2; dashed line, results for OCS; short-dashed line, results for CS_2.

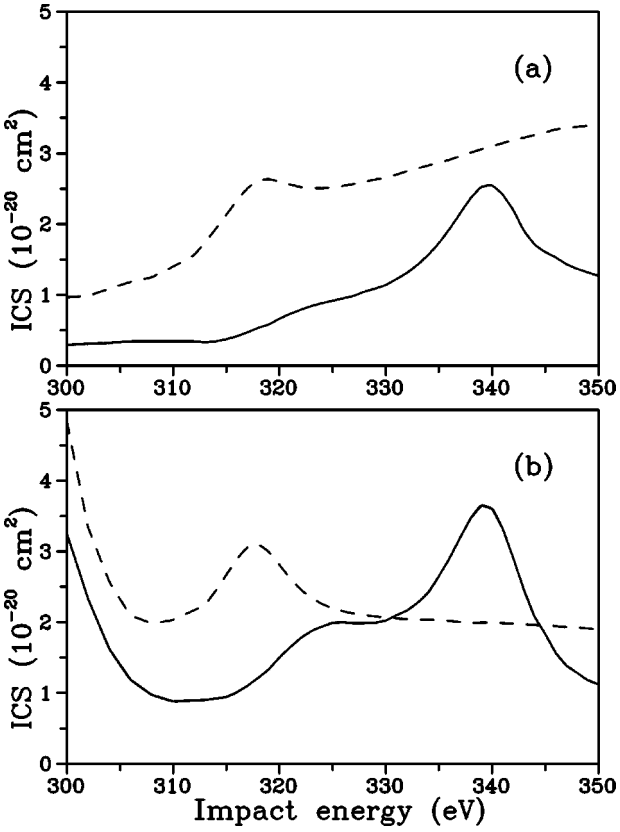

FIG. 6. Calculated partial ICS's for the two lowest e^--OCS scattering channels leading to (a) the singlet and (b) triplet excited states. Solid line, results for the $^2\Sigma$; dashed line, for the $^2\Pi$ scattering channels.

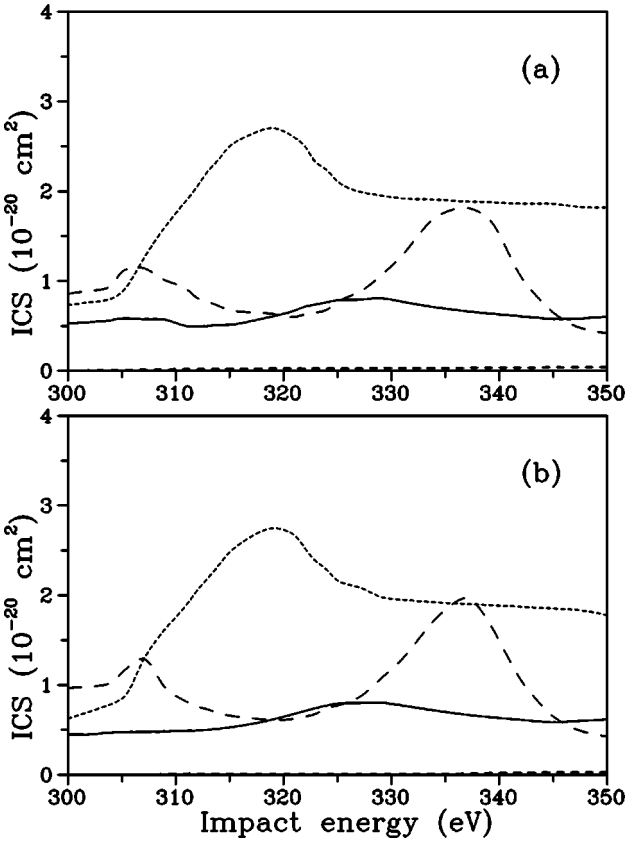

FIG. 7. Same as Fig. 4, but for e^--CS_2 scattering.

tations are shifted with each other. The singlet-triplet energy split is probably responsible for the shift. In contrast, no clear shift of the corresponding resonance positions is identified for singlet and triplet excitations in OCS and CS_2 due to the broadness of these structures in the calculated ICS's. Probably for this reason, no resonance structures are exhibited in the calculation of the RI(1:3) of the latter targets since the characteristic of resonances can be washed out by dividing the ICS's of the singlet excitation by those of the triplet excitation.

In summary, the present work reports a theoretical investigation on core-level ($C_{1s}\sigma \rightarrow \pi$) singlet and triplet transitions in CO_2, OCS, and CS_2 molecules. It is verified that the non-resonant excitations of these molecules are quite similar and are pratically independent of the excited valence orbital to which the core electron is promoted. This observation supports the expectation that the C(1*s*) electrons are in fact essentially *atomic* for these molecules. On the other hand, the resonant core-excitation processes of these targets are highly dependent on the chemical environment, i.e., the height and shape of the potential barrier of each target. This fact is evident by the width and intensity of the resonances in the calculated ICS's of the three target molecules studied here. In addition, the present work has shown that the occurrence of shape resonance, by itself, shall not ensure the exhibition of the resonance features in the RD(1:3) and RI(1:3). Instead, the width and the position shift of the corresponding resonances for singlet and triplet excitations are more decisive for their appearance in the experimental or calculated ratios. Based on this aspect, one might suspect that some resonances in electron-impact core-excitation processes could be missed in the measured ratios. Unfortunately, there are no experimental studies for CS_2 and OCS molecules reported in the literature.

Moreover, it is expected that the interesting features in electron-impact core excitation of the molecules studied here can also happen to other targets with at least one common atomic constituent. Efforts in this direction are underway.

ACKNOWLEDGMENTS

This research was partially supported by Conselho Nacional de Desenvolvimento Científico e Tecnológico (CNPq) and FAPESP.

[1] M.N. Piancastelli, J. Electron Spectrosc. Relat. Phenom. **100**, 167 (1999).
[2] C.R. Natoli, in *EXAFS and Near-Edge Structure*, edited by A. Bianconi, L. Incoccia, and S. Stipcich (Springer-Verlag, Berlin, 1983).
[3] J. Stöhr, J.L. Grand, W. Eberhardt, D. Outka, R.J. Madix, F. Sette, R.J. Koestner, and U. Doebler, Phys. Rev. Lett. **51**, 2414 (1983).
[4] J.L. Dehmer, J. Chem. Phys. **56**, 4496 (1972).
[5] J.L. Dehmer, D. Dill, and A.C. Parr, in *Photophysics and Photochemistry in the Vaccum Ultraviolet*, edited by S.P. McGlynn, G. Findley, and R. Huebner (Reidel, Dordrecht, 1985).
[6] V. McKoy, T.A. Carlson, and R.R. Lucchese, J. Chem. Phys. **88**, 3188 (1984).
[7] M.-T. Lee and K.T. Mazon, Phys. Rev. A **65**, 042720 (2002).
[8] F. Sette, J. Stöhr, and A.P. Hitchcock, Chem. Phys. Lett. **110**, 517 (1984).
[9] F. Sette, J. Stöhr, and A.P. Hitchcock, J. Chem. Phys. **81**, 4906 (1984).
[10] J.P. Zeisel, D. Teillet-Billy, L. Bouby, and R. Paineau, Chem. Phys. Lett. **63**, 47 (1979).
[11] D. Teillet-Billy and J.P. Zeisel, in *Proceedings of the 11th International Conference of Physics on Electronic and Atomic Collisions* (Society for Atomic Collision Research, Kyoto, 1979), Abstracts p. 404.
[12] I. Harrison and G.C. King, J. Phys. B **19**, L447 (1986).
[13] C.E. Blount and D.M. Dickinson, J. Electron Spectrosc. Relat. Phenom. **61**, 367 (1993).
[14] A.P. Hitchcook, S. Bodeur, and M. Tronc, Chem. Phys. **115**, 93 (1987).
[15] T. Kroin, S.E. Michelin, K.T. Mazon, D.P. Almeida, and M.-T. Lee, J. Mol. Struct.: THEOCHEM **464**, 49 (1999).
[16] T. Kroin, S.E. Michelin, and M.-T. Lee, J. Phys. B **34**, 1829 (2001).
[17] A.W. Fliflet and V. McKoy, Phys. Rev. A **21**, 1863 (1980).
[18] M.-T. Lee and V. McKoy, J. Phys. B **15**, 3971 (1982).
[19] M.-T. Lee, L.M. Brescansin, and M.A.P. Lima, J. Phys. B **23**, 3859 (1990).
[20] M.-T. Lee, S.E. Michelin, T. Kroin, L.E. Machado, and L.M. Brescansin, J. Phys. B **28**, 1859 (1995).
[21] R.R. Lucchese, G. Raseev, and V. McKoy, Phys. Rev. A **25**, 2572 (1982).
[22] T.H. Dunning, J. Chem. Phys. **55**, 716 (1971).
[23] S. Huzinaga, J. Chem. Phys. **42**, 202 (1956).
[24] M. Takekawa and Y. Itikawa, J. Phys. B **29**, 4227 (1996).
[25] P. Bündgen, F. Grein, and A.J. Thakkar, J. Mol. Struct.: THEOCHEM **334**, 7 (1995).
[26] M.-T. Lee, S.E. Michelin, T. Kroin, and E. Veitenheimer, J. Phys. B **32**, 3043 (1999).
[27] W.J. Hunt and W.J. Goddard, Chem. Phys. Lett. **24**, 464 (1974).
[28] H.M.B. Roberty, C.E. Bielschowsky, and G.G.B. Souza, Phys. Rev. A **44**, 1694 (1991).
[29] D.P. Almeida, G. Dawbwer, and G.C. King, Chem. Phys. Lett. **233**, 1 (1995).